Steps on $Fe_3O_4(100)$: STM measurements and theoretical calculations

Hui-Qiong Wang,[1] Eric I. Altman,[2] and Victor E. Henrich[1]
[1]*Department of Applied Physics, Yale University, P.O. Box 208284, New Haven, Connecticut 06520, USA*
[2]*Department of Chemical Engineering, Yale University, P.O. Box 208286, New Haven, Connecticut 06520, USA*
(Received 6 March 2006; revised manuscript received 17 April 2006; published 20 June 2006)

Scanning tunneling microscopy (STM) measurements of the step structure on natural single-crystal samples of $Fe_3O_4(100)$ have been performed. Step edges are found to occur along both [110] and $[1\bar{1}0]$ directions. For step heights of 4.2 ± 0.3 Å, the step edges are found to be straight, whereas for step heights of 2.1 ± 0.2 Å, alternate step edges are straight and jagged. The straight (jagged) step edges are parallel (perpendicular) to the octahedral iron rows on the upper terrace. The concepts of coordinative unsaturation and excess surface charge are used to predict which atomic geometries are likely to be most stable along step edges. Our calculations show that steps parallel to the octahedral iron rows on the upper terrace are expected to be more stable than those perpendicular to them, in agreement with our STM observations. This step stability is found to be independent of both terrace structure and step height.

DOI: 10.1103/PhysRevB.73.235418 PACS number(s): 68.35.Bs, 68.47.Gh, 68.37.Ef, 61.43.Bn

I. INTRODUCTION

The structure of the $Fe_3O_4(100)$ surface has been of increasing interest in the past few years, both because Fe_3O_4 is a metallic ferrimagnet that has potential applications in spintronics,[1] and because of the chemisorption behavior of Fe_3O_4.[2] Fe_3O_4 has the complex inverse spinel structure, based on a face-centered-cubic (fcc) oxygen sublattice, with the Fe cations occupying both octrahedral and tetrahedral lattice sites. Two-thirds of the Fe cations are Fe^{3+} and one-third are Fe^{2+}. All of the Fe^{2+} and half of the Fe^{3+} cations occupy octahedral sites, with the remaining Fe^{3+} cations in tetrahedral sites.[3] Figure 1 shows a side view of the Fe_3O_4 crystal structure; (100) planes are horizontal and into the page. There are two types of (100) planes: planes *A* containing only tetrahedrally coordinated Fe cations, and planes *B* composed of oxygen anions and octrahedrally coordinated Fe cations. Termination with either plane yields a polar surface,[4] and thus reconstruction would be necessary to produce a stoichiometric, charge-neutral surface structure.

The most commonly observed $Fe_3O_4(100)$ surface reconstruction found on both natural single crystals[5] and on Fe_3O_4 films grown by molecular beam expitaxy (MBE)[6–17] is $(\sqrt{2}\times\sqrt{2})R45°$. Both surface terminations have been proposed to explain the observed reconstruction. An *A*-terminated surface, proposed by Kim *et al.*,[7] where the surface charge is autocompensated due to half a monolayer of tetrahedral Fe vacancies, has been supported or used by other groups.[8,11,15,18–22] This model has been further modified to include relaxation of the tetrahedral ions in the first and third layers from a molecular dynamics calculation.[23] On the other hand, a *B*-terminated surface has also been proposed, where autocompensation is achieved by an array of oxygen vacancies and an associated change in the charges on the surface octahedral iron ions.[18,24] Charge ordering has also been proposed on a *B*-terminated surface, with the formation of Fe^{2+}-Fe^{2+} and Fe^{3+}-Fe^{3+} dimers, in order to interpret the observed scanning tunneling microscopy (STM) images.[25,26] Recent density functional theory (DFT) calculations also favor the *B*-plane termination with either an interlayer relaxation,[27] a wavelike surface structure,[28] or dimerization of the octrahedral Fe ions.[29]

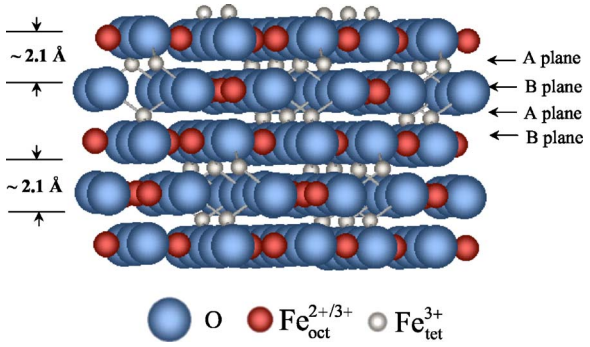

FIG. 1. (Color online) Side view of Fe_3O_4 with the (100) plane horizontal and into the page. The interlayer spacing between adjacent like planes (*A*-*A*, *B*-*B*) is ~2.1 Å.

Studies of the structure of steps on the $Fe_3O_4(100)$ surface are less extensive than are studies of the terrace structure. Only the step height between two adjacent terraces has been frequently reported to date. Most STM experiments reveal a minimum step height of about 2.1 Å,[5,6,11,12,18,25,26,30–38] corresponding to an interplanar spacing between two similar terraces, i.e., *A*-*A* planes or *B*-*B* planes (see Fig. 1). Occasionally, a minimum step height of 4.2 Å has been found,[25,39] corresponding to half of the bulk Fe_3O_4 unit cell. There is also one report of a step height of ~1 Å, indicating the coexistence of *A* and *B* terminations.[40] Mariotto *et al.*[32] and Ceballos *et al.*[34] mentioned that the step edges are straight along [110] and $[1\bar{1}0]$ directions. Gaines *et al.*[11] found that the image at the step edge is brighter than on the terraces and attributed it to either a step-edge reconstruction or a difference of the step-edge charge. Seoighe *et al.*[38] imaged straight step edges separated by a height of 2 Å as well as sawtooth edges separated by 1 Å. More recently, Subagyo and Sueoka[36] reported steps along the [110] direction with "poor straightness" resulting in irregularly shaped terraces. Studies of the atomic geometry along the step edges have never been reported, although step-edge ion sites are very important in chemisorption and catalysis.

To investigate the atomic geometry of steps on the $Fe_3O_4(100)$ surface, we present STM images taken on natural single-crystal samples and compare them to models of possible step structures. Two types of step edges are observed: straight step edges (α type) parallel to the octahedral iron rows on the upper terrace, and jagged step edges (β type) perpendicular to those rows. The concepts of coordinative unsaturation and excess surface charge are used to predict which atomic geometries are likely to be most stable along step edges.

II. EXPERIMENTAL DETAILS AND STM RESULTS

Natural Fe_3O_4 single crystals from the Jacupiranga mine, Sao Paulo, Brazil were used in this study. The (100) surface was oriented by Laue diffraction to within ±0.5° and cut into 1 mm thick, 1 cm diameter samples using a diamond saw. The samples were then polished mechanically using 3, 1, 0.3, and 0.05 μm aluminum oxide and subsequently cleaned in an ethanol ultrasonic bath before mounting onto a Mo sample holder and transfer into an ultrahigh-vacuum (UHV) system. The system consists of a single chamber equipped with low energy electron diffraction (LEED), Auger electron spectroscopy (AES), and STM. For STM measurements, electrochemically etched W tips were cleaned by electron bombardment prior to use; the tunneling current was kept between 0.1 and 1.0 nA, with most images taken using 0.5 nA.

The $Fe_3O_4(100)$ surface was prepared by first sputtering with 2 keV Ar^+ ions for 0.5 h, followed by 500 eV Ar^+ for 1 h to minimize the depth of sputter damage. After annealing at 873 K overnight, the surface displayed a $(\sqrt{2}\times\sqrt{2})$ $R45°$ reconstruction, as verified by LEED. Figure 2 shows STM images with step edges along [110] (a) and $[1\bar{1}0]$ (b). A line profile taken from *A* to *G* in Fig. 2(a) is shown in Fig. 2(c). The step heights from *E* to *F* and from *F* to *G* are both 4.2±0.3 Å, corresponding to half of the bulk Fe_3O_4 unit cell (two oxygen planes). Terrace edges separated by 4.2±0.3 Å are always observed to be straight. For two neighboring terraces separated by a step height of 2.1±0.2 Å (i.e., *B*-*C*, *C*-*D*, and *D*-*E*), one edge is straight and the adjacent one is jagged. The same pattern is shown in the top part of Fig. 2(b), where the step edges are rotated 90° from those in Fig. 2(a). A higher magnification image in Fig. 2(d) shows atom rows running in perpendicular directions on adjacent terraces that are separated by a step height of 2.1±0.2 Å. On each terrace, the distance between two adjacent rows is 5.9±0.6 Å, close to the inter-row spacing for the octahedral iron ions. A jagged step edge is highlighted by the black dashed line. This jagged step is perpendicular to the iron atom rows on the upper terrace (β type). Its adjacent step, whose height is 2.1±0.2 Å, is straight and runs parallel to the iron atom rows (α type).

III. THEORETICAL MODELING OF STEPS ON $Fe_3O_4(100)$

We can compare the stoichoimetry and charge state of different surface models by employing a method initially proposed by Finnis.[41] In order to calculate surface atom and

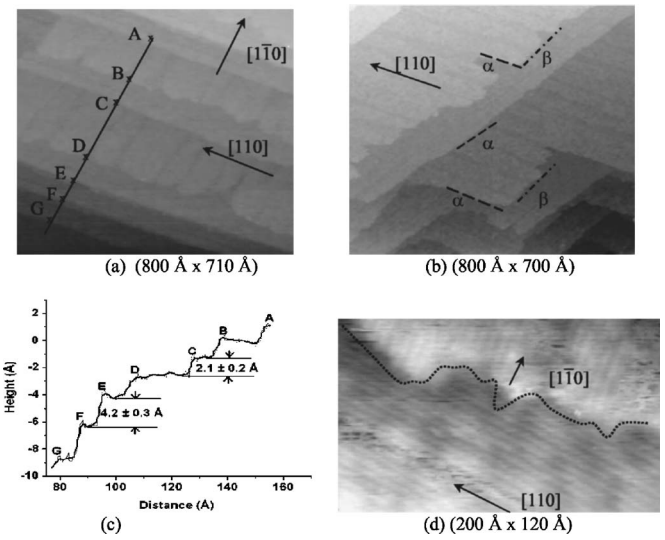

FIG. 2. STM images showing steps edges along [110] (a) and $[1\bar{1}0]$ (b). A line profile taken from *A* to *G* in (a) is shown in (c). The edges of two neighboring terraces separated by a step height of 4.2±0.3 Å are always straight. For those terraces separated by step heights of 2.1±0.2 Å, one edge is straight and the adjacent is jagged. A higher magnification image in (d) shows atom rows running in perpendicular directions on two adjacent terraces separated by a step height of 2.1±0.2 Å. The jagged pattern is indicated by the black dashed line. The symbols α and β shown in (b) correspond to two types of step models proposed in Sec. III. A tunneling current of 0.5 nA was used for all the images; the sample bias voltage was 1.50 V for (b) and 0.375 V for both (a) and (c).

charge excess, a definition of the "surface region" is required. However, different choices of surface boundaries generally lead to different results for many crystal structures. Finnis proposed a so-called weighted linear tapered termination, which results from averaging over an ensemble of different volumes for the surface region. Using this procedure, the results for surface charge excess and surface stoichiometry are independent of the choice of the plane separating the "surface" and "bulk" regions. That method of calculating charge excess has been extended by Henrich and Shaikhutdinov[2] to compute the atom and charge excess along surface steps for $Fe_3O_4(111)$. Here we use the method to determine the charge state of various step geometries for $Fe_3O_4(100)$.

Before calculating the step models for $Fe_3O_4(100)$, we applied Finnis's method to compute the atom and charge excess in the surface region for the various terrace models for $Fe_3O_4(100)$ that have been proposed (see Sec. I above). These include the "Fe_{tet}" model with a full *A*-plane termination; the "$1/2Fe_{tet}$" model, an *A*-plane termination with every other row of tetrahedral Fe^{3+} ions along [100] removed; the "O-Fe_{oct}" model exposing the ideal *B* plane; and the "O-Fe_{oct}+O_{vac}" model that removes 1/8 of the surface O anions. Our calculated results confirm that only the $1/2Fe_{tet}$ model is both stoichiometric and charge neutral, as proposed by Kim *et al.*;[7] none of the other models are either stoichiometric or charge neutral. Application of the atom and charge excess calculation to the models based on charge

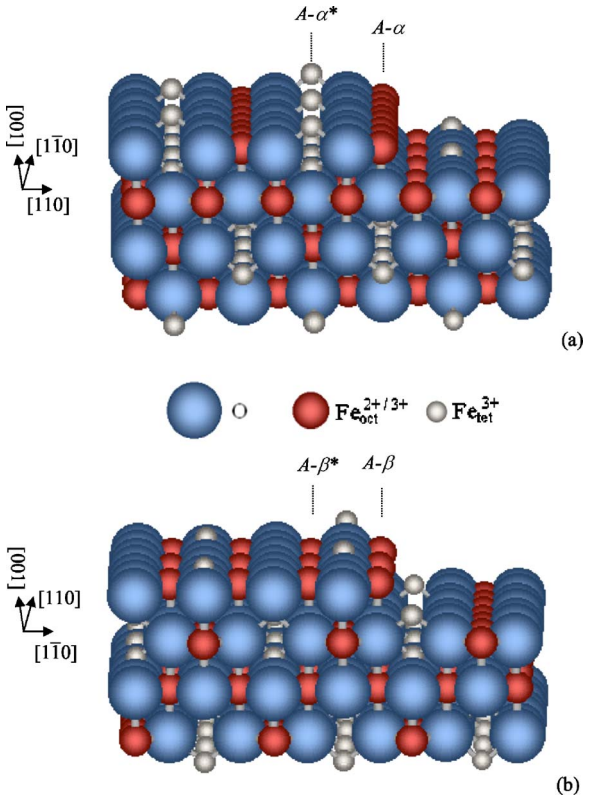

FIG. 3. (Color online) Step creation for the $1/2Fe_{tet}$ terrace. Steps can form along $[1\bar{1}0]$ (parallel to the iron ion rows) as A-α-type (a) or along [110] (perpendicular to the iron ion rows) as A-β-type (b).

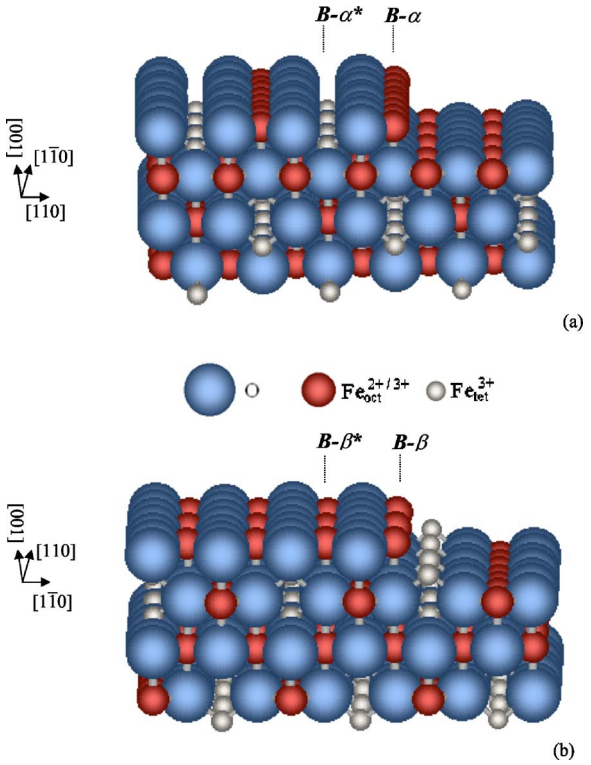

FIG. 4. (Color online) Step creation for the O-Fe_{oct} terrace: α type (a) and β type (b).

ordering[25,26] and those proposed by Cheng[27] and Pentcheva *et al.*[28] yield the same results as the O-Fe_{oct} model; Finnis's approach[41] is not able to address differences arising from charge ordering or structural relaxation.

Since the surface structure of $Fe_3O_4(100)$ is strongly dependent on the preparation procedure,[5] and since our STM images do not have sufficient resolution to determine the structural details, our $(\sqrt{2}\times\sqrt{2})$ $R45°$ surfaces could be either an A termination with the charge-neutral $1/2Fe_{tet}$ model, or a B termination with the wavelike pattern that has been found to be energetically stable.[28] We will use both terrace models for the step calculations. In Finnis's method, the wavelike model would be the same as the O-Fe_{oct} model. (We show later that the relative step stability does not depend on the terrace structure assumed.)

Our STM images show steps running along both [110] and $[1\bar{1}0]$ directions, with edges parallel (α-type step) or perpendicular (β-type step) to the octahedral iron atom rows of the upper terrace. α- and β-type steps would occur as alternate adjacent steps in a descending (or ascending) step structure having a step height of 2.1 Å. Figure 3(a) indicates the two possible planes along which an α step can be created on a surface having the $1/2Fe_{tet}$ terrace structure, labeled "A-α" and "A-α^*". Similarly, Fig. 3(b) shows the two options for generating β steps, indicated as "A-β" and "A-β^*". Creation of the α- and β-type steps for the O-Fe_{oct} terrace structure is illustrated in Figs. 4(a) and 4(b), respectively.

For each of the four step planes above, different atomic configurations along the step edge are possible, depending on which Fe atoms are removed in creating the step. These different configurations have very different excess charge and coordinative unsaturation, which is crucially important in chemisorption and catalysis [see, for example, Ref. 2 for chemisorption at steps on the $Fe_3O_4(111)$ surface]. As in Ref. 2, our criterion is that any Fe atom missing more than half of its O ligands will be removed from the step, since it should not be stable there. For example, Fig. 5 shows the three step structures that result for B-α steps. The full row of octrahedral Fe cations can remain (B-α-1), or half of them can be removed (B-α-2) without altering the size of the step unit cell. One can also consider removing all of the step-edge Fe cations (B-α-3). Applying these criteria results in nine possible step structures for the $1/2Fe_{tet}$ surface and eight for the O-Fe_{oct} surface.

The atomic bonding in Fe_3O_4 is partly covalent and partly ionic. In order to determine the most stable step geometry, we consider both surface ion coordinative unsaturation (covalent stability) by counting dangling bonds, and the criterion of charge neutrality (ionic stability) by calculating the charge excess along a step. The same unit cell is chosen for all steps having the O-Fe_{oct} surface terrace; its length is two O atoms along the step, and it includes from the row of O atoms along the edge of the top terrace down to the first row of O atoms on the lower terrace in front of the step. That cell is the smallest one that contains all of the atoms whose ligand coordinations might change as cations are removed from the step. The numbers of short (tetrahedral) and long (octahedral) dangling bonds for each step are given in Tables I and II, as are the "effective" total number of dangling bonds/cell, tabulated both as in Refs. 42 and 43. (See Ref. 2

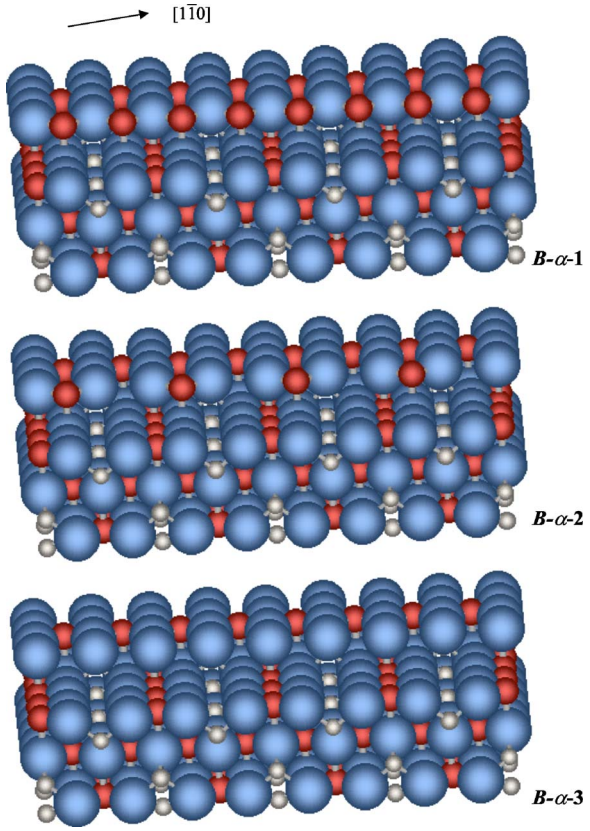

FIG. 5. (Color online) Three possible B-α-type step models for the O-Fe_{oct} terrace.

for details of dangling bond determination and the relative weighting of short and long bonds.) The step unit cell for steps having the $1/2Fe_{tet}$ surface terrace has a length of four O atoms along the steps, twice that of steps having the O-Fe_{oct} surface terrace. In Table I, the number of dangling bonds and the excess charge for the $1/2Fe_{tet}$ terrace steps has been divided by 2 so that all step models can be quantitatively compared.

To calculate the charge excess for the step models, a tapered termination is chosen parallel to the surface terraces and terminating near the step edge. Figure 6 shows the tapered volume for a B-α-1 step. The volume runs from right to left and contains two planes of oxygen ions into the page. The number of each type of atom per unit cell in each vertical plane is determined, and each plane is given a weight, w, inversely proportional to its distance from an atomic plane chosen as the beginning of the tapered termination; any planes beyond the starting plane are given weights of 1. [As mentioned above, the step unit cell for the $1/2Fe_{tet}$ terrace structure is twice as large as that for the O-Fe_{oct} terrace. Also, in order to construct a stoichiometric unit cell (a requirement for Finnis's method), the half monolayer of Fe_{tet} ions in the outermost plane, the second layer of O and Fe_{oct} ions, and half of the Fe_{tet} ions in the third layer are included.]

With appropriate charge(s) assigned to the cations and anions, the positive charge excess of this surface, $[N_+/N_-]$, is given by

$$[N_+/N_-] = \frac{\begin{vmatrix} [N_+] & [N_-] \\ N_+ & N_- \end{vmatrix}}{N_-}, \tag{1}$$

where $[N_+]=\Sigma n_+ w=$ the total weighted number of positive charges in tapered termination, $[N_-]=\Sigma n_- w=$ the total weighted number of negative charges in tapered termination, $N_+=$ the actual number of positive charges in one (sub)unit cell of the crystal, and $N_-=$ the actual number of negative charges in one (sub)unit cell of the crystal.

Since the tapered volume requires at least one stoichiometric repeat unit of the crystal structure, N_+ will always be equal to N_-. Thus, Eq. (1) can be further simplified to

$$[N_+/N_-] = [N_+] - [N_-]. \tag{2}$$

It is not possible to uniquely determine the amount of electronic charge associated with a particular ion in any material. So any calculation of excess charge on a surface or along a step relies on a *model* for the charges on the ions

TABLE I. Summary of step stability criteria for $Fe_3O_4(100)$ with a $1/2Fe_{tet}$ terrace.

			Dangling bonds/ half-step unit cell		Excess charge/half step unit cell (unit |e|)			
Step	Tet. bonds	Oct. bonds	1 short =1.5 long	1 short =1.8 long	Model 1	Model 2	Model 3 ×(16/13)	Average of Models 1–3
A-α-1	0	4	4	4	+2.67	+2.5	+2.46	+2.54±0.09
A-α-2	0	5	5	5	0	0	0	0±0
A-α-3	0	6	6	6	−2.67	−2.5	−2.46	−2.54±0.09
A-α^*-1	1.5	0	2.25	2.7	0	0	0	0±0
A-α^*-2	1	0	1.5	1.8	−0.67	−0.75	−0.77	−0.73±0.05
A-β-1	0	2	2	2	+1.33	+1.25	+1.23	+1.27±0.05
A-β-2	0	3	3	3	−1.33	−1.25	−1.23	−1.27±0.05
A-β^*-1	0	2	2	2	+1.33	+1.25	+1.23	+1.27±0.05
A-β^*-2	0	3	3	3	−1.33	−1.25	−1.23	−1.27±0.05

TABLE II. Summary of step stability criteria for Fe_3O_4(100) with a O-Fe_{oct} terrace.

Step	Tet. bonds	Oct. bonds	Dangling bonds/ step unit cell: 1 short =1.5 long	Dangling bonds/ step unit cell: 1 short =1.8 long	Excess charge/step unit cell (unit |e|): Model 1	Model 2	Model 3 ×(16/13)	Average of Models 1–3
B-α-1	0	4	4	4	+2.67	+2.5	+2.46	+2.54±0.09
B-α-2	0	5	5	5	0	0	0	0±0
B-α-3	0	6	6	6	−2.67	−2.5	−2.46	−2.54±0.09
B-α^*	1	0	1.5	1.8	+1.33	+1.5	+1.54	+1.46±0.09
B-β-1	0	2	2	2	+0.67	+0.5	+0.46	+0.54±0.09
B-β-2	0	3	3	3	−2	−2	−2.0	−2±0
B-β^*-1	0	2	2	2	+2	+2	+2.0	+2±0
B-β^*-2	0	3	3	3	−0.67	−0.5	−0.46	−0.54±0.09

involved. We use the same three models to assign charges to the cations and anions for Fe_3O_4 as in Ref. 2 and references therein. Two of the models arbitrarily assign the O anions a fully ionic charge of −2, which essentially ignores any covalent component to the interatomic bonding. One of these models (Model 1) then assigns all of the Fe cations an average charge of +8/3, as was done in Ref. 42. The other (Model 2) gives the tetrahedral Fe cations a charge of +3, and the octrahedral Fe cations an average charge of +2.5, as in Ref. 43, since half of the octahedral cations have a formal valence of +3, while the other half are +2. Another approach (Model 3) is to explicitly assume partial covalent bonding by reducing the charge on both cations and anions.[44] We arbitrarily reduce the charge on the Fe_{tet} ions from +3 to +2.5, and reduce the Fe_{oct} cations from +2.5 to +2. The stoichiometry of Fe_3O_4 dictates that the O ions must have a charge of −1.625 in order to maintain charge neutrality in the bulk. However, for this choice, the bulk unit cell contains only 13/16 of the charge in Models 1 and 2, so to compare the three models below, we must multiply the charges given by Model 3 by 16/13.

The number of dangling bonds/step unit cell and the excess charge/step unit cell for all the step geometries and charge models considered are presented in Table I for the $1/2Fe_{tet}$ terrace and Table II for the O-Fe_{oct} terrace. Notice that the choice of ionic charge makes little difference in the amount of excess step charge, and *no* difference in the ordering of values for different steps. In Table I, two of the α-type steps, *A*-α-2 and *A*-α^*-1, are charge neutral, while another, *A*-α^*-2, has the smallest number of dangling bonds; similarly in Table II, one of the α-type steps, *B*-α-2, is charge neutral and another, *B*-α^*, has the smallest number of dangling bonds. Figure 7 shows the atomic structure for the three charge-neutral steps. None of the β-type steps in either table is charge neutral, and they all have similar numbers of dangling bonds. The different number of dangling bonds and different excess charge on steps having different cation configurations would presumably lead to very different chemisorption and catalytic behavior, although that has not yet been studied for stepped Fe_3O_4(100).

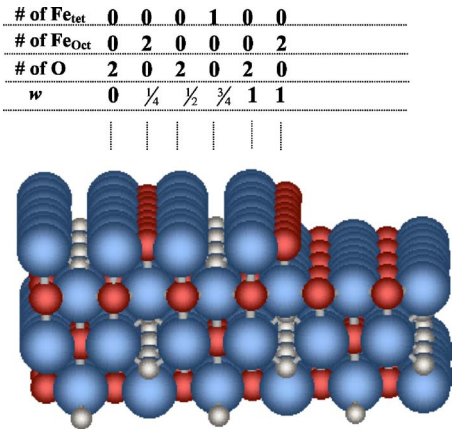

FIG. 6. (Color online) Model of a *B*-α-1 step (into the page) on the Fe_3O_4(100) surface for computing atom excess.

For Fe_3O_4(100), the conditions of covalent stability—minimize dangling bonds—and ionic stability—minimize excess charge along steps—yield different answers for which specific step model is expected to be most stable: step *A*-α^*-2 and *B*-α^* have the smallest numbers of dangling bonds, while steps *A*-α-2, *A*-α^*-1, and *B*-α-2 are the only charge-neutral steps. This is different from the results found for steps on Fe_3O_4(111), where the same step structures met both stability criteria.[2]

Some degree of reconstruction or relaxation is expected whenever dangling bonds are present on a surface. In metal oxides, partially coordinated surface cations often relax into the underlying oxygen plane in order to reduce their coordinative unsaturation.[45] Adjacent dangling bonds may also form surface dimers, as occurs for semiconductor surfaces. Either of these effects would lead to a smaller effective number of surface dangling bonds than those given in Tables I and II. Such reconstruction or relaxation may also be accompanied by a redistribution of charge among ions in the surface region. That redistribution would not, however, change the overall charge balance in the surface region, so the method of evaluating excess surface charge used here would still give the correct answer. Therefore, we speculate that the ionic stability criteria should be more reliable than the cova-

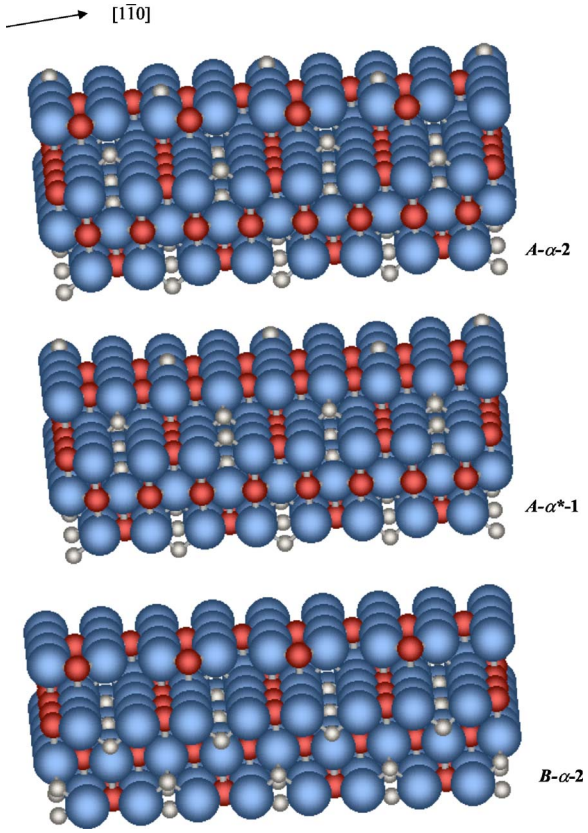

FIG. 7. (Color online) Three α-type charge-neutral step models.

lent stability criteria used here. This reasoning leads to α-type steps being more stable than β types for a step height of 2.1 Å with either the $1/2Fe_{tet}$ or the O-Fe_{oct} surface termination.

We have also performed charge excess calculations on step models with a step height of 4.2 Å with the O-Fe_{oct} terrace structure. Using the same step creation criteria leads to ten models for α-type steps and nine for β types. The calculations show that there are five almost charge-neutral, double-height steps, where four are α-type steps and only one is a β-type step. So, as for 2.1 Å height steps, it would be more likely to have α-type, double-height steps.

The conclusions drawn above suggest an explanation for our experimental STM data (see Fig. 2). For steps separated by a step height of 2.1 ± 0.2 Å, the two step edges should correspond to one α type and one β type; one step edge is observed to be straight and the other jagged. The straight step edges are parallel to the octahedral iron rows on the upper terrace and are thus α-type steps. The adjacent step edges are β-type steps.

These β-type steps exhibit a large number of kinks. The edges of the kinks and the trenches, which are oriented 90° to the β-type step direction, would be α type. For steps separated by a step height of 4.2 ± 0.3 Å, both step edges would correspond to the same type of step model (either α type or β type); such steps are observed to be straight, with edges running parallel to the octahedral iron rows on the upper terrace. These are thus α-type steps, in agreement with our calculations. Both the experiment and calculations show that α-type steps are more stable than β type, regardless of the step height.

The step structure seen on $Fe_3O_4(100)$ is similar to that found on some semiconductor surfaces; alternating jagged and smooth steps have been reported for $Si(100)(2\times1)$.[46,47] For Si, the origin is attributed to different step energies depending on whether the steps are parallel or perpendicular to the dimer rows on the terrace. Steps that have higher step energies are also found to have higher kink densities. We also see a much lower kink density along α-type steps than along β-type steps. However, atomic bonding in Si is purely covalent, so a direct comparison with Fe_3O_4 cannot be made.

IV. SUMMARY

We have studied steps on the $Fe_3O_4(100)$ surface by using both STM measurements on natural single-crystal samples and by computing charge and atom excesses for various step geometry models. STM images show steps oriented along both [110] and [1$\bar{1}$0] directions. For step heights of 4.2 ± 0.3 Å, all step edges are straight, whereas for step heights of 2.1 ± 0.2 Å, straight edges alternate with jagged ones. Both the $1/2Fe_{tet}$ and O-Fe_{oct} terrace models have been used for the calculation of the stability of possible step geometries along both the [110] and [1$\bar{1}$0] directions. Steps along the [1$\bar{1}$0] direction, parallel to the octahedral iron rows on the upper terrace, are found to be more stable than the steps along the [110] direction. This result is in good agreement with our STM observations and is found to be independent of the terrace model assumed. The step stability criterion is also independent of the step height.

ACKNOWLEDGMENTS

This research is partially supported by U.S. Department of Energy Grant No. DE-FG02-00ER45844, NSF Equipment Grant No. DMR-0075824, and NSF Grant MRSEC DMR-0520495. E.I.A. also acknowledges the support of the Petroleum Research Foundation Grant No. 41278-AC5. The authors thank W. Gao, J. Wang, and M. Li for their assistance in carrying out this work, and S. Ismail-Beigi for helpful discussions.

[1] S. A. Wolf, D. D. Awschalom, R. A. Buhrman, J. M. Daughton, S. von Molnar, M. L. Roukes, A. Y. Chtchelkanova, and D. M. Treger, Science **294**, 1488 (2001).
[2] V. E. Henrich and S. K. Shaikhutdinov, Surf. Sci. **574**, 306 (2005).
[3] J. B. Goodenough, in *Metallic Oxides*, edited by H. Reiss (Pergamon, New York, 1972). [Prog. Solid State Chem. **5**, 145 (1972).]

[4] P. W. Tasker, J. Phys. C **12**, 4977 (1979).
[5] G. Tarrach, D. Burgler, T. Schaub, R. Wiesendanger, and H.-J. Güntherodt, Surf. Sci. **285**, 1 (1993).
[6] S. A. Chambers and S. A. Joyce, Surf. Sci. **420**, 111 (1999).
[7] Y. J. Kim, Y. Gao, and S. A. Chambers, Surf. Sci. **371**, 358 (1997).
[8] S. A. Chambers, S. Thevuthasan, and S. A. Joyce, Surf. Sci. **450**, L273 (2000).
[9] F. C. Voogt, T. T. M. Palstra, L. Niesen, O. C. Rogojanu, M. A. James, and T. Hibma, Phys. Rev. B **57**, R8107 (1998).
[10] F. C. Voogt, T. Hibma, G. L. Zhang, M. Hoefman, and L. Niesen, Surf. Sci. **333**, 150 (1995).
[11] J. M. Gaines, P. J. H. Bloemen, J. T. Kohlhepp, C. W. T. Bulleieuwma, R. M. Wolf, A. Reinders, R. M. Jungblut, P. A. A. van der Heijden, J. T. W. M. van Eemeren, J. aan de Stegge, and W. J. M. de Jonge, Surf. Sci. **373**, 85 (1997).
[12] A. Subagyo, K. Sueoka, and K. Mukasa, J. Magn. Magn. Mater. **290**, 1037-1039 (2005).
[13] Y. Gao, Y. J. Kim, and S. A. Chambers, J. Mater. Res. **13**, 2003 (1998).
[14] T. Hibma, F. C. Voogt, L. Niesen, P. A. A. van der Heijden, W. J. M. de Jonge, J. J. T. M. Donkers, and P. J. van der Zaag, J. Appl. Phys. **85**, 5291 (1999).
[15] J. F. Anderson, M. Kuhn, U. Diebold, K. Shaw, P. Stoyanov, and D. Lind, Phys. Rev. B **56**, 9902 (1997).
[16] J. Korecki, B. Handke, N. Spiridis, T. Slezak, I. Flis-Kabulska, and J. Haber, Thin Solid Films **412**, 14 (2002).
[17] Y. Gao and S. A. Chambers, J. Cryst. Growth **174**, 446 (1997).
[18] B. Stanka, W. Hebenstreit, U. Diebold, and S. A. Chambers, Surf. Sci. **448**, 49 (2000).
[19] D. O. Boerma, Nucl. Instrum. Methods Phys. Res. B **183**, 73 (2001).
[20] L. A. Kalev, P. Schurer, and L. Niesen, Phys. Rev. B **68**, 165407 (2003).
[21] A. V. Mijiritskii, M. H. Langelaar, and D. O. Boerma, J. Magn. Magn. Mater. **211**, 278 (2000).
[22] A. V. Mijiritskii and D. O. Boerma, Surf. Sci. **486**, 73 (2001).
[23] J. R. Rustad, E. Wasserman, and A. R. Felmy, Surf. Sci. **432**, L583 (1999).
[24] F. C. Voogt, T. Fujii, P. J. M. Smulders, L. Niesen, M. A. James, and T. Hibma, Phys. Rev. B **60**, 11193 (1999).
[25] R. Wiesendanger, I. V. Shvets, D. Bürgler, G. Tarrach, H. J. Güntherodt, J. M. D. Coey, and S. Gräser, Science **255**, 583 (1992).
[26] G. Mariotto, S. Murphy, and I. V. Shvets, Phys. Rev. B **66**, 245426 (2002).
[27] C. Cheng, Phys. Rev. B **71**, 052401 (2005).
[28] R. Pentcheva, F. Wendler, H. L. Meyerheim, W. Moritz, N. Jedrecy, and M. Scheffler, Phys. Rev. Lett. **94**, 126101 (2005).
[29] I. V. Shvets, G. Mariotto, K. Jordan, N. Berdunov, R. Kantor, and S. Murphy, Phys. Rev. B **70**, 155406 (2004).
[30] J. M. Gaines, J. T. Kohlhepp, P. J. H. Bloemen, C. W. T. Bulleieuwma, R. M. Wolf, A. Reinders, and R. M. Jungblut, J. Magn. Magn. Mater. **165**, 439 (1997).
[31] K. Jordan, G. Mariotto, S. F. Ceballos, S. Murphy, and I. V. Shvets, J. Magn. Magn. Mater. **290&291**, 1029 (2005).
[32] G. Mariotto, S. F. Ceballos, S. Murphy, and I. V. Shvets, J. Appl. Phys. **93**, 7142 (2003).
[33] H.-Q. Wang, W. Gao, E. I. Altman, and V. E. Henrich, J. Vac. Sci. Technol. A **22**, 1675 (2004).
[34] S. F. Ceballos, G. Mariotto, S. Murphy, and I. V. Shvets, Surf. Sci. **523**, 131 (2003).
[35] N. Spiridis, B. Handke, T. Slezak, J. Barbasz, M. Zajac, J. Haber, and J. Korecki, J. Phys. Chem. B **108**, 14356 (2004).
[36] A. Subagyo and K. Sueoka, Jpn. J. Appl. Phys., Part 1 **44**, 5447 (2005).
[37] M. Fonin, R. Pentcheva, Y. S. Dedkov, M. Sperlich, D. V. Vyalikh, M. Scheffler, U. Rüdiger, and G. Güntherodt, Phys. Rev. B **72**, 104436 (2005).
[38] C. Seoighe, J. Naumann, and I. V. Shvets, Surf. Sci. **440**, 116 (1999).
[39] R. Koltun, M. Herrmann, G. Güntherodt, and V. A. M. Brabers, Appl. Phys. A: Mater. Sci. Process. **73**, 49 (2001).
[40] S. F. Ceballos, G. Mariotto, K. Jordan, S. Murphy, C. Seoighe, and I. V. Shvets, Surf. Sci. **548**, 106 (2004).
[41] M. W. Finnis, Phys. Status Solidi A **166**, 397 (1998).
[42] A. Barbieri, W. Weiss, M. A. Van Hove, and G. A. Somorjai, Surf. Sci. **302**, 259 (1994).
[43] M. Ritter and W. Weiss, Surf. Sci. **432**, 81 (1999).
[44] K. Hermann and M. Scheffler (private communication).
[45] V. E. Henrich and P. A. Cox, *The Surface Science of Metal Oxides* (Cambridge University Press, 1994).
[46] H. J. W. Zandvliet, H. B. Elswijk, E. J. van Loenen, and D. Dijkkamp, Phys. Rev. B **45**, 5965 (1992).
[47] B. S. Swartzentruber, Y.-W. Mo, R. Kariotis, M. G. Lagally, and M. B. Webb, Phys. Rev. Lett. **65**, 1913 (1990).